ChemComm

Accepted Manuscript

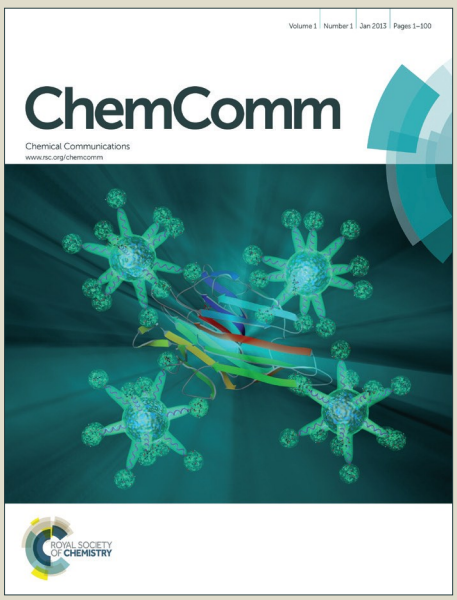

This is an *Accepted Manuscript*, which has been through the Royal Society of Chemistry peer review process and has been accepted for publication.

Accepted Manuscripts are published online shortly after acceptance, before technical editing, formatting and proof reading. Using this free service, authors can make their results available to the community, in citable form, before we publish the edited article. We will replace this *Accepted Manuscript* with the edited and formatted *Advance Article* as soon as it is available.

You can find more information about *Accepted Manuscripts* in the Information for Authors.

Please note that technical editing may introduce minor changes to the text and/or graphics, which may alter content. The journal's standard Terms & Conditions and the Ethical guidelines still apply. In no event shall the Royal Society of Chemistry be held responsible for any errors or omissions in this *Accepted Manuscript* or any consequences arising from the use of any information it contains.

ROYAL SOCIETY OF CHEMISTRY

www.rsc.org/chemcomm

Please do not adjust margins

ChemComm

ARTICLE

Fluorescent supramolecular nanoparticles signal the loading of electrostatically charged cargo

Received 00th January 20xx,
Accepted 00th January 20xx

DOI: 10.1039/x0xx00000x

www.rsc.org/

Laura Grana Suarez, Willem Verboom* and Jurriaan Huskens*

Fluorescently labeled supramolecular nanoparticles (SNPs) were used to study the effects of their loading with oppositely charged cargo. SNPs shrank until neutralization, upon which they destabilized and aggregated. Using a dye-labelled guest, FRET occurred between the SNPs and a dye-labeled cargo. This effect may allow the development of responsive imaging and drug delivery vehicles.

Supramolecular nanoparticles (SNPs) are formed by specific non-covalent interactions in a multicomponent system.[1] The toolbox approach of SNPs, in which multivalent and monovalent building blocks are assembled in a one-pot process, presents many advantages such as size control, controlled assembly/disassembly, modular exchange of building blocks with desired properties, and easy incorporation of imaging agents or targeting ligands.[1] SNPs are therefore being studied for various biomedical applications, such as imaging,[2] photothermal therapy,[3] drug delivery,[4-8] and gene delivery.[9,10]

The loading of drugs or nucleic acid derivatives into SNPs can be achieved by different strategies, e.g., by host-guest chemistry[10-15] or electrostatics.[5,12,16-19] The latter approach is used extensively in the case of electrostatically charged guests, such as charged drugs. SNPs for the delivery of RNA or DNA constitute a clear example of this approach: the genetic material is negatively charged, and for this reason it needs a positively charged scaffold to be encapsulated.[9-11,16] The components of the SNPs can be charged as desired: negatively, as in the system recently developed in our group which makes use of the biocompatible poly(isobutyl-*alt*-maleic acid) (PiBMA) polymer,[20] or positively, such as in the systems of Tseng[4] and Davis,[16] in which cyclodextrin (CD)-grafted poly(ethylene imine) (PEI) has been used. In Tseng's system, the SNP formation is governed by CD host-guest interactions, and the role of electrostatics remains often subdued. In contrast, in Davis' system, the electrostatics between the CD-PEI and the DNA/RNA payload is the main SNP driving force, and the CD host-guest interactions are merely used for the attachment of the monovalent stopper which provides SNP stabilization. Both systems have been studied extensively in terms of particle formation, release of the cargo, optimum ratio of scaffold/cargo, and toxicology.[9,12,13,17,19,21,22] Although the effects of the charged cargo on the particle characteristics and stability are of utmost importance for biomedical applications, these aspects have hardly been explored so far.

Fluorescence spectroscopy is a powerful and sensitive technique, and has been used, amongst others, for the study of supramolecular assemblies for sensing and on-off switching.[23-25] Forster Resonance Energy Transfer (FRET) describes the process by which the excitation energy is transferred from one dye to another that is in close proximity, and this process is widely used for the study of conformational changes in assemblies and biomolecular systems.[26-30] Moreover, the quenching of fluorescent polymers (superquenching) has appeared as an emergent technique to study DNA hybridization, and to detect a variety of biological targets.[26,31-34] Fluorescence techniques thus can offer unique ways to explore the changes occurring in SNPs upon addition of a guest. Using charged SNPs that have been equipped with a fluorescent dye, the addition of a complementary charged guest, with or without a dye that forms a FRET couple with the first dye, may alter the characteristics of the particles and affect the fluorescence properties of the SNPs. Therefore, we envisage that fluorescence and FRET methods will allow the study of the loading of guests into SNPs.

Here, we aim to study the effects of loading a charged fluorescent cargo into charged fluorescent SNPs held together by cyclodextrin (CD) host-guest interactions, thus changing the electrostatic environment of the particles, on the SNP properties, such as size and stability. Also, the changes in the fluorescent properties of the assemblies, such as self-quenching and energy transfer of the FRET couple, will act as a tool for studying these assemblies. The SNPs are characterized by DLS and zeta potential, while cargo loading is studied by monitoring the changes in UV and fluorescence properties upon the addition of cargo.

The components used to form the fluorescent SNPs and their self-assembly are shown in Fig. 1. Guest loading into the SNPs (Fig. 1a) is studied by interacting a fluorescently labelled

[a] *Molecular Nanofabrication group, MESA+ Institute for Nanotechnology, University of Twente, P.O. Box 217, 7500 AE Enschede, The Netherlands. E-mail: w.verboom@utwente.nl & j.huskens@utwente.nl; Fax: +31-534894645*

Electronic Supplementary Information (ESI†) available: Synthesis and characterization of the polymers, protocol of the preparation of the particles, characterization of the particles (DLS, HRSEM, UV-Vis and fluorescence spectroscopy), controls. See DOI: 10.1039/x0xx00000x

ChemComm Accepted Manuscript

Please do not adjust margins

polymeric cationic guest with SNPs that contain a fluorescent dye-modified anionic polymeric building block. As a consequence, the overall particle charge is expected to change from negative to neutral and ultimately positive upon increase of the cationic guest concentration. These changes of the electrostatic properties are expected to affect the fluorescence characteristics of the particles (Fig. 1a,b). Furthermore, fluorescein (FL) and rhodamine B (RhB), the two dyes used to tag the cargo and the labelled SNP building block, form a FRET couple, which is used here to study proximity effects within the SNPs.

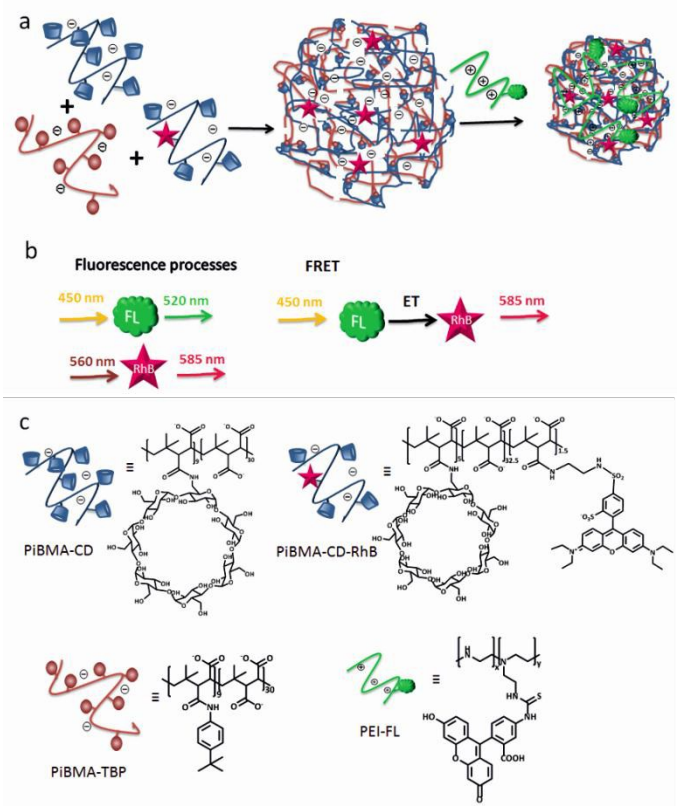

Fig. 1 (a) Self-assembly of the components to form the fluorescent SNPs and their loading with a charged cargo. (b) Fluorescence and FRET processes used here. (c) Components of the SNP system: host polymer grafted solely with CD (PiBMA-CD), host polymer grafted with CD and lissamine rhodamine B (PiBMA-CD-RhB), guest polymer grafted with *p–tert*-butyl-phenyl groups (PiBMA-TBP), and the cargo polymer poly(ethylene imine) grafted with fluorescein (PEI-FL).

The host and the guest polymers (Fig. 1b,c), cyclodextrin-grafted poly(isobutyl-*alt*-maleic acid) (PiBMA-CD) and *p-tert*-butylphenyl-grafted PiBMA (PiBMA-TBP), were synthesized as described before,[20,35-37] and contained, on average, 9 CD units and 9 TBP units per polymer backbone, respectively. The host polymer grafted with rhodamine (PiBMA-CD-RhB) was synthesized in a stepwise process by amidation of poly(isobutyl-*alt*-maleic anhydride) (MW 6 kDa) with lissamine™ rhodamine B ethylenediamine followed by 6-monodeoxy-6-monoamino-β-cyclodextrin (see ESI†). The positively charged cargo polymer, poly(ethylene imine) (PEI) grafted with fluorescein (FL), was synthesized by thiourea bond formation by reaction of PEI with fluorescein isothiocyanate (see ESI†). The crude products were purified by dialysis and neutralized before freeze-drying. ^{1}H-NMR (Fig. S1, ESI†) analysis of PiBMA-CD-RhB revealed that it contained, on average, 5 CD moieties per polymer backbone, as determined by comparing the methyl signals of the polymer with the H1-CD signal of the CD moieties. PiBMA-CD-RhB was grafted with, on average, 1.5 RhB per polymer backbone, and PEI-FL with 0.3 FL per polymer backbone as determined by UV analysis (see calibration curves in Fig. S2, ESI†). The host polymer with/without dye (PiBMA-CD-RhB, PiBMA-CD) and the guest polymer (PiBMA-TBP) formed fluorescent SNPs in phosphate buffer (5 mM, pH 7.4, Fig. 1a) stabilized by a balance between attractive supramolecular host-guest interactions between CD and TBP and repulsive electrostatic interactions between the polymer chains, without the need of a monovalent stopper, as studied before for the parent system without RhB label.[20] The ratio between PiBMA-CD and its dye-modified counterpart PiBMA-CD-RhB was used to control the dye concentration. The cargo PEI, unlabelled or labelled with FL, was added after SNP formation, and it was incorporated in the SNP core (Fig. 1a) by attractive electrostatic interactions with the host and guest polymers. The concentration of PEI was determined based on its molecular weight, and, therefore, on the number of polymer chains.

The change of the SNP particle size upon addition of increasing amounts of (unlabelled) PEI was monitored by dynamic light scattering (DLS). As shown in Fig. 2a, the particles shrank upon the first addition to approx. half of their original size. This size was maintained until reaching a concentration of 2.3 µM PEI, at which further increase of the concentration led to the formation of large aggregates. Although a size decrease upon loading cargo might seem counterintuitive at first, it must be noted that the electrostatic repulsive interactions between the SNP building blocks provides the SNPs with an open, hydrogel-like structure. Loading with oppositely charged cargo therefore reduces the repulsion and thus causes shrinkage of the SNPs, with concurrent loss of water from the SNP core.

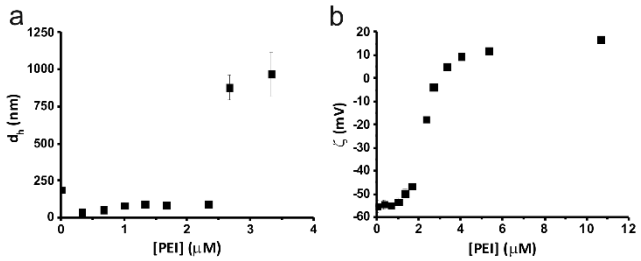

Fig. 2 (a) Hydrodynamic diameters from DLS and (b) zeta potential (ζ) data of the SNPs composed of PiBMA-CD-RhB (3.3 µM CD, 1 µM RhB), PiBMA-CD (11.7 µM CD) and PiBMA-TBP (15 µM TBP) upon addition of increasing amounts of PEI.

A similar transition was observed by zeta potential (ζ) measurements (Fig. 2b) which showed that, upon addition of PEI, the charge of the SNPs gradually became less negative. In the case of using PEI-FL as the cargo, comparable results were obtained (Fig. S3, ESI†). At a concentration of 2.3 µM PEI, the point of neutralization was reached, and the particles became positively charged at higher amounts of cargo. However, the absolute value of the zeta potential remained below 20 mV, which is in agreement with the loss of colloidal stability as

ChemComm Accepted Manuscript

This journal is © The Royal Society of Chemistry 20xx

observed by DLS. Moreover, the maintained, low positive charge at high cargo concentrations indicates that guest uptake beyond the point of neutralization is increasingly hampered by electrostatic repulsion.

Comparing the amounts of positive and negative charges present in the SNPs upon addition of PEI/PEI-FL to the preformed particles indicates that the particles reach the point of neutralization at a concentration of 2.3 μM PEI/PEI-FL (the theoretical calculation of the neutralization point together with the assumptions made are given in the ESI†, Table S1). This agrees well with the experimental DLS and zeta potential data shown in Fig. 2. Lindman and coworkers have observed a similar aggregation behavior for particles formed by condensates of DNA and a polyelectrolyte.[38,39] In a previous study,[20] we observed that the negatively charged SNPs are stabilized by a balance between attractive supramolecular and repulsive electrostatic forces. Whenever this equilibrium is perturbed, for example by exposing the particles to high ionic strength, or by addition of a charged cargo as done here, the particles destabilize and aggregate. Thus, as indicated by the zeta potential and DLS measurements, the cargo-loaded SNPs lose their colloidal stability when reaching the point of neutralization.

The optical properties of the cargo-loaded SNPs were studied by UV-Vis absorption and fluorescence spectrophotometry (Fig. 3) using the RhB-labelled component PiBMA-CD-RhB in SNP formation (Fig. 1). In the UV-Vis spectra (Fig. 3a), a Mie scattering component started to appear upon reaching a cargo (PEI) concentration of 2.3 μM, suggesting the presence of large aggregates. As described above, this cargo concentration coincides with the point of neutralization, leading to loss of colloidal stability. The fluorescence emission intensity of RhB upon excitation of RhB at 560 nm of SNPs containing PiBMA-CD-RhB upon addition of PEI or PEI-FL is shown in Fig. 3b (fluorescence emission spectra in Fig. S4, ESI†). The addition of the cargo to the SNPs caused a continuous decrease in the RhB emission, attributed to self-quenching of RhB, until the neutralization point was reached at a concentration of 2.5 μM PEI/PEI-FL, upon which the intensity started to level off. The increased quenching of the RhB emission can in part be attributed to shrinking of the SNPs, which brings the dyes closer together, as observed as well by DLS, although the particles shrink sharply upon addition of cargo, while the quenching happens gradually. Additionally, the increasing amounts of charges upon cargo loading may increase the polar nature of the SNP core promoting aggregation of the dye moieties of both the SNP building blocks and the cargo. Upon reaching the point of neutralization, the influx of cargo is largely inhibited, as observed as well by the zeta potential measurements, and consequently the fluorescence intensity levels off. In the case of PEI-FL, the quenching of RhB appeared to be more effective (Fig. 3b) due to the presence of increasing amounts of FL into the SNPs, which contribute to the dye aggregation and, therefore, to the extent of self-quenching of RhB, and possibly FRET (see below). These results clearly indicate that the SNPs have become responsive to cargo loading upon the use of a fluorescent dye as a label at one of the SNP components.

The particles were imaged by high-resolution scanning electron microscopy (HR-SEM). Fig. 4 shows images of SNPs after addition of PEI-FL, at concentrations before (Fig. 4a) or after (Fig. 4b) the point of neutralization. Fig. 4a displays round, well defined small particles of approx. 50 nm in size, whereas in Fig. 4b large, amorphous aggregates are clearly visible. The original particles before adding the cargo (Fig. S5, ESI†) were 70 nm, comparable to the size obtained for the parent SNPs without RhB.[20] This shows that the particles shrink in size, when cargo is added before reaching the point of neutralization, as shown before by DLS, although the size difference by SEM is less evident than by DLS. Beyond the point of neutralization, the particles destabilize and form aggregates, probably by the merging of several particles.

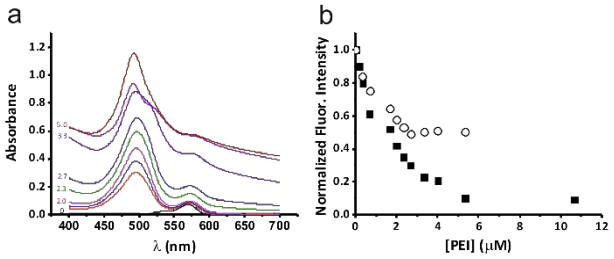

Fig. 3 (a) UV/Vis absorbance spectra, and (b) normalized fluorescence intensities (excitation of RhB at 560 nm, emission of RhB at 585 nm) of SNPs composed of PiBMA-CD-RhB (3.3 μM CD, 1 μM RhB), PiBMA-CD (11.7 μM CD) and PiBMA-TBP (15 μM TBP) upon addition of increasing amounts of PEI (b, ○) or PEI-FL (a and b, ▪). The standard deviation of the normalized fluorescence intensities was on average 0.02.

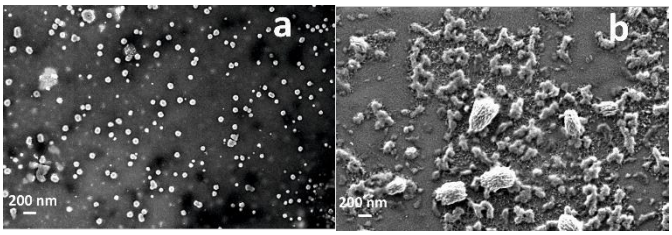

Fig. 4 HR-SEM images of the SNPs composed of PiBMA-CD-RhB (3.3 μM CD, 1 μM RhB), PiBMA-CD (11.7 μM CD) and PiBMA-TBP (15 μM TBP) after adding (a) 0.67 or (b) 5.33 μM PEI-FL.

As a control, SNPs of unlabelled PiBMA-CD were prepared and free RhB was added at the same dye concentration as for the dye-labelled SNPs shown in Fig. 3, after which free fluorescein with or without PEI was added. In both cases, quenching of RhB was no longer observed (Fig. S6a, ESI†). This indicates that RhB must be incorporated inside the SNPs, by covalent attachment to one of its constituents, to be able to observe quenching due to the loading of cargo. Similarly, when free FL was added to the RhB-labelled SNPs prepared with PiBMA-CD-RhB, quenching of RhB was also not observed (Fig. S6b, ESI†). However, quenching did take place once PEI was also added, which indicates that the quenching of RhB originates from the charge neutralization induced by the cationic cargo.

FRET occurring between the fluorescein and rhodamine B dyes was studied by monitoring the fluorescence emission of RhB at 585 nm of SNPs upon excitation of FL at 450 nm upon addition of PEI-FL or PEI, as is shown in Fig. 5a (fluorescence emission spectra in Fig. S7, ESI†). When the particles were loaded with PEI-FL, an increase of the fluorescence emission of RhB was observed, indicating FRET from FL to RhB. The effect occurred until the point of neutralization at 2.5 μM, which indicates that beyond this concentration no more PEI-FL was

ChemComm Accepted Manuscript

loaded into the SNPs. Once the charges are compensated, there is no driving force to encapsulate more PEI-FL, and, consequently, the increase of the FRET effect levels off. In the case of unlabelled PEI as the cargo, no emission of RhB was observed under the same conditions, indicating that FRET is only observed when FL is attached to the cargo. Fig. 5b shows the fluorescence emission of the PEI-FL cargo at 520 nm when administered to the SNPs or to the buffer solution without SNPs, upon excitation of FL at 450 nm. The intensity increase upon increasing amounts of PEI-FL in the presence of RhB-labelled SNPs was slightly lower than in the absence of SNPs, which confirms FRET from FL to RhB in the cargo-loaded SNPs. As a negative control, Fig. 5b also shows the intensities upon loading unlabelled PEI as a cargo to RhB-labelled SNPs. The absence of fluorescence confirms that the emission observed in the former cases is fully attributable to FL emission. Overall, the fluorescence properties of both dyes clearly indicate that FRET occurs between the dye-labelled SNP components and the dye-labelled cargo.

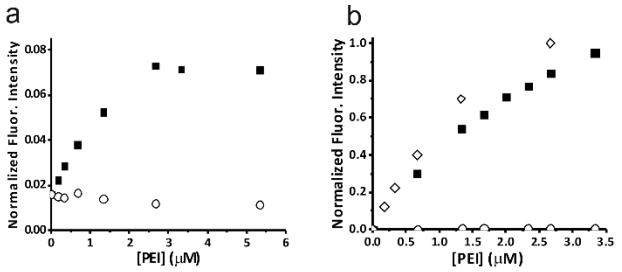

Fig. 5 Fluorescence emission intensity of the SNPs composed of PiBMA-CD-RhB (3.3 μM CD, 1 μM RhB), PiBMA-CD (11.7 μM CD) and PiBMA-TBP (15 μM TBP) after adding PEI-FL or PEI. (a) Excitation of FL at 450 nm, emission of RhB at 560 nm (normalized to the maximum intensity of the emission of RhB obtained after its direct excitation; see Fig. 3). (b) Excitation of FL at 450 nm, emission of FL at 520 nm (normalized to the fluorescence intensity of FL with free PEI-FL at 2.7 μM PEI); ▪ SNPs to which PEI-FL was added. ○ SNPs to which PEI was added. ◊ free PEI-FL. The standard deviation of the normalized fluorescence intensities was on average 0.001 in (a) and 0.02 in (b).

In conclusion, we have developed a fluorescent multicomponent supramolecular nanoparticle system that is responsive to the loading of cargo. Equipment of one the SNP components with a fluorescent reporter dye allowed us to study the effect on the particle behaviour and stability upon the introduction of oppositely charged cargo. Particle destabilization and aggregation occurred once the neutralization point was reached. Before the neutralization point, the cargo loading caused shrinkage of the SNPs. When both the SNPs and the cargo were labelled with a dye, FRET was observed upon loading the SNPs with cargo. These results further the basic understanding of the forces underlying SNP morphology and stability when loading SNPs with an electrostatically charged cargo, such as in the case of anticancer gene delivery. Moreover, the counteracting fluorescence intensities of the SNP components and the cargo, caused by FRET, may allow the development of drug delivery vehicles and imaging agents in which the ratiometric detection[40,41] of the dye intensities can be used to signal the SNP assembly and disassembly, as well as the release of cargo.

Mark Smithers is acknowledged for the recording of the HRSEM images. This work was supported by the Dutch Technology Foundation STW (NWO-nano, project number 11435).

Notes and References

1 K.-J. Chen, M. A. Garcia, H. Wang and H.-R. Tseng, *Supramolecular Chemistry*, John Wiley & Sons, Ltd, 2012.
2 H. Wang, S. T. Wang, H. Su, K. J. Chen, A. L. Armijo, W. Y. Lin, Y. J. Wang, J. Sun, K. Kamei, J. Czernin, C. G. Radu and H. R. Tseng, *Angew. Chem., Int. Ed.*, 2009, **48**, 4344.
3 S. Wang, K.-J. Chen, T.-H. Wu, H. Wang, W.-Y. Lin, M. Ohashi, P.-Y. Chiou and H.-R. Tseng, *Angew. Chem., Int. Ed.*, 2010, **49**, 3777.
4 J.-H. Lee, K.-J. Chen, S.-H. Noh, M. A. Garcia, H. Wang, W.-Y. Lin, H. Jeong, B. J. Kong, D. B. Stout, J. Cheon and H.-R. Tseng, *Angew. Chem., Int. Ed.*, 2013, **52**, 4384.
5 K.-J. Chen, L. Tang, M. A. Garcia, H. Wang, H. Lu, W.-Y. Lin, S. Hou, Q. Yin, C. K. F. Shen, J. Cheng and H.-R. Tseng, *Biomaterials*, 2012, **33**, 1162.
6. Q.-L. Li, W.-X. Gu, H. Gao and Y.-W. Yang, *Chem. Commun.*, 2014, **50**, 13201.
7. W.-X. Gu, Q.-L. Li, H. Lu, L. Fang, Q. Chen, Y.-W. Yang and H. Gao, *Chem. Commun.*, 2015, **51**, 4715.
8. Y. Wu, Y. Long, Q.-L. Li, S. Han, J. Ma, Y.-W. Yang and H. Gao, *ACS Appl. Mater. Interfaces*, 2015, **7**, 17255.
9 M. E. Davis, *Mol. Pharmaceutics*, 2009, **6**, 659.
10 M. E. Davis, *Adv. Drug Delivery Rev.*, 2009, **61**, 1189.
11 S. Gaur, Y. Wang, L. Kretzner, L. Chen, T. Yen, X. Wu, Y.-C. Yuan, M. Davis and Y. Yen, *Nanomed. Nanotech.*, 2014, **10,** 1477.
12 Q. D. Hu, H. Fan, Y. Ping, W. Q. Liang, G. P. Tang and J. Li, *Chem. Commun.*, 2011, **47**, 5572.
13 F. Zhao, H. Yin and J. Li, *Biomaterials*, 2014, **35**, 1050.
14 W. Bouquet, W. Ceelen, B. Fritzinger, P. Pattyn, M. Peeters, J. P. Remon and C. Vervaet, *Eur. J. Pharm. Biopharm.*, 2007, **66**, 391.
15 F. Fenyvesi, T. Kiss, É. Fenyvesi, L. Szente, S. Veszelka, M. A. Deli, J. Váradi, P. Fehér, Z. Ujhelyi, Á. Tósaki, M. Vecsernyés and I. Bácskay, *J. Pharm. Sci.*, 2011, **100**, 4734.
16 M. E. Davis, J. E. Zuckerman, C. H. J. Choi, D. Seligson, A. Tolcher, C. A. Alabi, Y. Yen, J. D. Heidel and A. Ribas, *Nature*, 2010, **464**, 1067.
17 Y. Liu, H. Wang, K.-i. Kamei, M. Yan, K.-J. Chen, Q. Yuan, L. Shi, Y. Lu and H.-R. Tseng, *Angew. Chem., Int. Ed.*, 2011, **50**, 3058.
18 C. Aranda, K. Urbiola, A. Méndez Ardoy, J. M. García Fernández, C. Ortiz Mellet and C. T. de Ilarduya, *Eur. J. Pharm. Biopharm.*, 2013, **85**, 390.
19 Q. Hu, W. Li, X. Hu, Q. Hu, J. Shen, X. Jin, J. Zhou, G. Tang and P. K. Chu, *Biomaterials*, 2012, **33**, 6580.
20 L. Grana Suarez, W. Verboom and J. Huskens, *Chem. Commun.*, 2014, **50**, 7280.
21 H. Wang, K.-J. Chen, S. Wang, M. Ohashi, K.-i. Kamei, J. Sun, J. H. Ha, K. Liu and H.-R. Tseng, *Chem. Commun.*, 2010, **46**, 1851.
22 A. Méndez-Ardoy, N. Guilloteau, C. Di Giorgio, P. Vierling, F. Santoyo-González, C. Ortiz Mellet and J. M. García Fernández, *J. Org. Chem.*, 2011, **76**, 5882.
23 J. Mohanty, N. Thakur, S. Dutta Choudhury, N. Barooah, H. Pal and A. C. Bhasikuttan, *J. Phys. Chem. B*, 2011, **116**, 130.
24 M. Shaikh, S. D. Choudhury, J. Mohanty, A. C. Bhasikuttan and H. Pal, *Phys. Chem. Chem. Phys.*, 2010, **12**, 7050.
25 R. N. Dsouza, U. Pischel and W. M. Nau, *Chem. Rev.*, 2011, **111**,7941
26 K. E. Sapsford, L. Berti and I. L. Medintz, *Angew. Chem., Int. Ed.*, 2006, **45**, 4562.
27 S. Ghosh, C. Ghosh, S. Nandi and K. Bhattacharyya, *Phys. Chem. Chem. Phys.*, 2015, **17**, 8017.
28 X. Zhou, X. Wu and J. Yoon, *Chem. Commun.*, 2015, **51**, 111.
29 S. Tyagi and E. A. Lemke, *Curr. Opin. Struct. Biol.*, 2015, 32, 66-73.
30 T. A. Theodossiou, A. R. Gonçalves, K. Yannakopoulou, E. Skarpen and K. Berg, *Angew. Chem., Int. Ed.*, 2006, **45**, 4562.
31 S. Kumaraswamy, T. Bergstedt, X. Shi, F. Rininsland, S. Kushon, W. Xia, K. Ley, K. Achyuthan, D. McBranch and D. Whitten, *P. Natl. Acad. Sci. USA.*, 2004, **101**, 7511.
32 S. A. Kushon, K. Bradford, V. Marin, C. Suhrada, B. A. Armitage, D. McBranch and D. Whitten, *Langmuir*, 2003, **19**, 6456.
33 S. A. Kushon, K. D. Ley, K. Bradford, R. M. Jones, D. McBranch and D. Whitten, *Langmuir*, 2002, **18**, 7245.
34 S. W. Thomas Iii, J. P. Amara, R. E. Bjork and T. M. Swager, *Chem. Commun.*, 2005, **36**, 4572.
35. M. Weickenmeier, G. Wenz and J. Huff, *Macromol. Rapid Comm.*, 1997, **18**, 1117.
36. B. J. Ravoo, J.-C. Jacquier and G. Wenz, *Angew. Chem., Int. Ed.*, 2003, **42**, 2066.
37. M. Klink and H. Ritter, *Macromol. Rapid Comm.*, 2008, **29**, 1208-1211.
38 M. Cardenas, K. Schillen, T. Nylander, J. Jansson and B. Lindman, *Phys. Chem. Chem. Phys.*, 2004, **6**, 1603.
39 D. Lundberg, A. M. Carnerup, J. Janiak, K. Schillén, M. da Graça Miguel and B. Lindman, *Phys. Chem. Chem. Phys.*, 2011, **13**, 3082.
40 M. D. Yilmaz, S.-H. Hsu, D. N. Reinhoudt, A. H. Velders and J. Huskens, *Angew. Chem., Int. Ed.*, 2010, **49**, 5938.
41 R. V. Søndergaard, N. M. Christensen, J. R. Henriksen, E. K. P. Kumar, K. Almdal and T. L. Andresen, *Chem. Rev.*, 2015, **115**, 8344.

ChemComm Accepted Manuscript

This journal is © The Royal Society of Chemistry 20xx

Fluorescent supramolecular nanoparticles signal the loading of electrostatically charged cargo

Laura Grana Suarez, Willem Verboom* and Jurriaan Huskens*

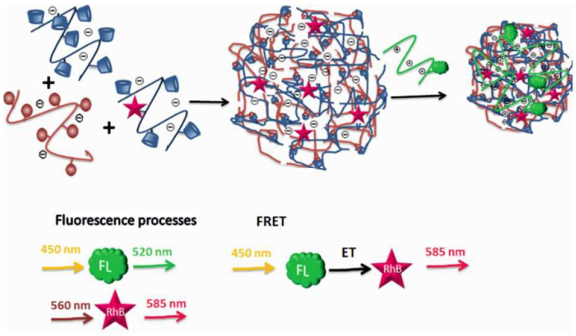

Supramolecular nanoparticles (SNPs) become responsive to the loading of cargo by attaching a fluorescent dye to one of the building blocks. The SNPs shrink upon loading them with a positively charged cargo polymer. When using a dye-labeled cargo, FRET occurs between the SNP components and the cargo.

ChemComm Accepted Manuscript